J Electr Eng Technol.2016; 11(5): 1077-1083
http://dx.doi.org/10.5370/JEET.2016.11.5.1077

ISSN(Print) 1975-0102
ISSN(Online) 2093-7423

Integration of Energy Storage for Voltage Support in Distribution Systems with PV Generation

Mohamed Shaaban† and J .O. Petinrin*

Abstract – The exploitation of PV generation offers substantial environmental benefits. Yet, the integration of these might be problematic due to its variable and intermittent nature. Energy storage can compensate for the deficiencies featured by variable PV systems. This paper provides a mathematical programming based approach for the strategic deployment of energy storage in the feeder circuits to achieve ubiquitous grid benefits. A genetic algorithm (GA) is used to solve the problem of appropriate size and location of the energy storage. Quasi-static time sequence analysis is carried out on diurnal basis, to correlate the coincidence of the PV resource output and demand. This will ensure accurate appraisal of storage impacts on the system hour by hour. The proposed approach is implemented on the IEEE 123 node test feeder under various penetration levels and operating scenarios. Results have consistently affirmed that the proposed approach is efficient in maintaining system's voltage profile at various conditions as well as reducing the overall thermal losses.

Keywords: Distribution system, Energy storage, Generic algorithms, Photovoltaic (PV) generation, Smart grid, Voltage control

1. Introduction

With the tendency to integrate higher penetration levels of PV generation into the distribution system, traditional downstream flow of power in feeder circuits can be reversed, with the possibility of injecting power back to the transmission network [1]. The consequences of such massive integration of PV generation will not only turn the passive distribution system into an active network, but also may bring about some critical operational issues to distribution system operators (DSOs) as far as voltage, frequency, reactive power, and protection coordination are concerned [2]. The variable nature of solar irradiance, resulting in intermittent output energy, could well lead to voltage rise, particularly when PV generation is high and demand is low [3].

Deployment of energy storage (ES) throughout the grid from generation to end-users presents an opportunity to transcend the real-time power balance paradigm between supply and demand. Since the solar peak takes place two to three hours earlier than customer peak load, energy can be stored at solar peak, with less line losses, and re-dispatched later when needed at customer peak loading. Energy storage was reportedly used with small solar arrays to even out the power flow as clouds pass over, and in ancillary service provision, such as frequency regulation [4].

Voltage rise mitigation, due to the connection of large amounts of distributed generators to medium (MV)/low voltage (LV) distribution networks, using load tap-changing transformer (LTC), was addressed in [5]. Through finding the value of the reactive power needed to minimize the voltage rise, the LTC is controlled to adjust the voltage settings. However, the volatility of tap positions becomes higher using this approach and feeder losses increase as well. Additionally, tuning the LTC will affect all feeders supplied by the same transformer and the amount of reactive power required will significantly swell with higher penetration levels. Besides, not all LV distribution networks are equipped with the LTCs.

Utilization of the ES can also be productive to reduce voltage rise problems. Among the main issues related to the integration of the ES into the distribution system, is its proper size and strategic location [6, 7]. An iterative procedure to derive a voltage sensitivity matrix for a grid feeder was developed to identify critical storage locations with respect to load/generation conditions [8]. However, the use of single point in time or snapshot load flow analysis is inadequate, since active and reactive power flow directions in the network can change at any instant due to the intermittency of PV generation.

An OPF-based algorithm for allocating the aggregated capacity size of the ES to determine the amount of spilled wind energy, with an objective to minimize annual electricity costs, was developed in [9]. Nevertheless, using the highest amount of curtailed wind as the aggregate magnitude of the storage is circumstantial. It also restricts the benefit of the ES to circumventing energy spillage only, ignoring other system-wide contributions towards thermal loss reduction, regulation requirements and upgrade

† Corresponding Author: Department of Electrical Engineering, Faculty of Engineering, Port Said University, Port Fouad 42523, Port Said, Egypt. (m.shaaban@ieee.org)
* Electrical/Electronic Engineering Department, School of Engineering, Federal Polytechnic Ede, Osun State, Nigeria. (wolepet01@yahoo.com)
Received: January 19, 2015; Accepted: March 16, 2016

deferral; to name a few.

Conventional optimization techniques start with an arbitrary single candidate solution and search iteratively for the optimal solution based on a specific criterion. Dissimilar to these, genetic algorithms (GAs) uses a population of candidate solutions to search multiple areas of the search space simultaneously based on a stochastic criterion. They are usually capable of achieving high quality solutions within reasonable execution time [10].

A matrix real-coded GA technique was proposed to optimally coordinate the power production of DGs and energy storage to minimize the operational costs of a microgrid [11]. A neural network was used to forecast the energy output of the PV sources, and battery storage was modeled aggregately. The paper, however, assumes identical batteries based on the size of the PV system. In other words, the magnitude and position of the ES were not studied.

A heuristic tool using the GA with simulated annealing was described in [12], to locate distributed ES in LV networks. Monte Carlo simulations were utilized to randomly site the PV systems at full power and the highest voltage is determined. The heuristic tool is then applied to find out the storage needed. Nonetheless, a single time step load flow is performed to evaluate the worst-case scenario.

This paper does not only investigate the use of the ES in PV generation capacity firming and output smoothing, but also as a viable tool for system-wide voltage support. Unlike snapshot analysis that does not reflect the value of time; the procedure used in the paper contemplates the time-integral part of the power flow including intermittent PV generation and typical changing load demand. The problem of sizing and allocating the ES is described as a nonlinear mathematical programming problem to minimize voltage variations and energy losses, while considering bus voltage magnitudes, and the ES physical limits. GA is employed to determine the optimal size and location of the ES to preserve system voltage profile against intermittent characteristics of solar-fueled generation. A quasi-static time sequence analysis simulation is carried out on the IEEE 123 test feeder system to verify the effectiveness of the proposed approach.

2. Problem Formulation

Energy storage provides multifaceted opportunities for significant benefits to electric energy supply, ancillary services, utility customers, grid system, and integration of renewables [4]. The key function of the ES in modern distribution systems is, however, to counterpoise the intermittency introduced by connecting solar-fueled generation at the point of common coupling (PCC). Such effect of the ES is likely to reduce the overall losses and support the system voltage profile. Therefore, the problem of finding the optimal site and capacity of the ES can be cast as a mathematical programming problem, where the objective is to minimize hourly energy losses and voltage deviations across all network nodes. This can be expressed mathematically as:

$$\text{Min } F = w_v \sum_{i=1}^{N}\sum_{t=1}^{24}\left\|V_{i,t} - V_{ref}\right\|^2 + w_l \sum_{i=1}^{N}\sum_{t=1}^{24} P_{L_{i,t}} \Delta t \qquad (1)$$

where w_v and w_l are the weighted-coefficients of voltage minimization and loss minimization respectively. $V_{i,t}$ and V_{ref} are the voltage of bus i at time t and magnitude of voltage reference respectively, obtained from the distribution power flow. V_{ref} is considered unity in this paper. $P_{L,t}$ is the network loss at time t. Δt is 1 hour time interval and N is the number of buses.

The first term of (1), corresponds to the squared norm of voltage deviations over the given period of time, whereas the second term represents the total network losses at time t.

The sum of the total power losses due to the ES is given as [13]:

$$P_{Li,t} = \sum_{j=1}^{N}\begin{bmatrix}\alpha_{ij,t}\left(P_{i,t}P_{j,t} + Q_{i,t}Q_{j,t}\right) \\ +\beta_{ij,t}\left(Q_{i,t}P_{j,t} + P_{i,t}Q_{j,t}\right)\end{bmatrix} \qquad (2)$$

where

$$\alpha_{ij} = \frac{r_{ij}}{V_{i,t}V_{j,t}}\cos\left(\delta_{i,t} - \delta_{j,t}\right)$$

$$\beta_{ij} = \frac{r_{ij}}{V_{i,t}V_{j,t}}\sin\left(\delta_{i,t} - \delta_{j,t}\right)$$

and

$Z_{ij} = r_{ij} + x_{ij}$ is the ijth element of [$Zbus$] matrix.

$P_{i,t} = P_{PV_{i,t}} \pm P_{ES_{i,t}} - P_{D_{i,t}}$, $Q_{i,t} = Q_{PV_{i,t}} \pm Q_{ES_{i,t}} - Q_{D_{i,t}}$

$P_{i,t}$ and $Q_{i,t}$ are the net active and reactive power injections at bus i at time t, $P_{PVi,t}$ and $Q_{PVi,t}$ are the active and reactive powers generated from PV generators at time t. $P_{ESi,t}$ and $Q_{ESi,t}$ are the active and reactive power produced/absorbed by the ES at bus i at time t, while $P_{Di,t}$ and $Q_{Di,t}$ are the load active and reactive powers at bus i at time t respectively.

The constraints include power flow equality constraints which can be represented as:

$$P_{i,t} = V_{i,t}\sum_{j=1}^{N} V_{j,t}\begin{bmatrix}G_{i,j}\cos\left(\delta_{i,t} - \delta_{j,t}\right) \\ +B_{i,j}\sin\left(\delta_{i,t} - \delta_{j,t}\right)\end{bmatrix} \qquad (3)$$

$$Q_{i,t} = V_{i,t}\sum_{j=1}^{N} V_{j,t}\begin{bmatrix}G_{i,j}\sin\left(\delta_{i,t} - \delta_{j,t}\right) \\ -B_{i,j}\cos\left(\delta_{i,t} - \delta_{j,t}\right)\end{bmatrix} \qquad (4)$$

where $V_{j,t}$ is the voltage at bus j at time t, $G_{i,j}$ and $B_{i,j}$ are the conductance and susceptance of the line between buses i and j respectively, whereas $\delta_{i,t}$ is the voltage angle at bus i at time t.

Voltage limits:

$$V_{\min} \le V_{i,t} \le V_{\max} \tag{5}$$

Storage physical and operating limits:

$$\sum_{t=1}^{24} -P_{ES_{i,t}} \Delta t \eta_i \le E_{ES_i}^{\max} - E_{ES_i}^{0} \tag{6}$$

$$\sum_{t=1}^{24} P_{ES_{i,t}} \Delta t \eta_i \le E_{ES_{i,t}}^{0} \tag{7}$$

$$E_{ES_i}^{\min} \le E_{ES_{i,t}} \le E_{ES_i}^{\max} \tag{8}$$

$$P_{ES_i}^{\min} \le P_{ES_{i,t}} \le P_{ES_i}^{\max} \tag{9}$$

Power loss constraint:

$$P_{Li,t}^{\text{with ES}} \le P_{Li,t}^{\text{without ES}} \tag{10}$$

where η is the energy storage round-trip efficiency, E_{ES} is the energy stored in the ES, and E^{0}_{ESi} is the initial energy stored at bus i, where the ES is located. E^{max} and E^{min} are maximum and minimum energy capacity of the storage respectively. P^{max} and P^{min} are maximum and minimum MW capacity of the storage respectively.

Eqs. (6) and (7) denote the maximum and minimum amount of the energy charged or discharged from the ES respectively. Similarly, (8) and (9) are the maximum and minimum ES capacity with the relevant active power rating. Eq. (10) guarantees that, incorporation of the ES improves the system-wide losses.

The formulation from (1) to (10) gives a complete description for the modeling of energy storage required to mitigate the impact of the PV generation on system losses and voltage profile. To avoid multi-objective programming, weights are assigned to objective function components [14]. Each objective function is multiplied by scalar weighting factors. The weighting factors are usually normalized as:

$$\sum_{k=1}^{K} W_k = 1 \tag{11}$$

Therefore; $w_v + w_l = 1$.

3. Genetic Algorithm (GA) Implementation

Genetic algorithms (GAs) belong to the class of Metaheuristics that maintains multiple chromosomes of individual solutions. Thus, they can explore wider areas of the search space, where the probability of finding improved solutions is high. One of the attractive properties of the GA is its ability to solve multidimensional, non-differentiable, and non-continuous complex problems, as well as the rapid discovery of good solutions. Among the caveats to GA implementation is that there is no absolute assurance the resulting solution is a global optimal. Nonetheless, GA-based solutions usually have good engineering accuracy and are amenable to parallel implementation, which can be useful to reduce the computational requirements [10].

Sizing the ES and allocating it into the distribution system represents a large-scale, combinatorial, nonlinear optimization problem. Picking out the node number, where the storage should be connected at, is inherently an integer problem.

GA starts with a randomly generated population; each representing a possible solution. Each individual string, composed of node locations and maximum capacity, is evaluated and assigned a fitness value, which indicate the relative quality of the potential solution. The fitness function used to evaluate the candidate strings is:

$$\text{Fitness} = -\left[w_v \sum_{i=1}^{N} \sum_{t=1}^{24} \left\| V_{i,t} - V_{ref} \right\|^2 + w_l \sum_{i=1}^{N} \sum_{t=1}^{24} P_{L_{i,t}} \right] \tag{12}$$

Constraint handling is carried out through penalty functions to penalize chromosomes that violate the constraints. Genetic operators are then applied to diversify the solution and produce good potential solutions. A new

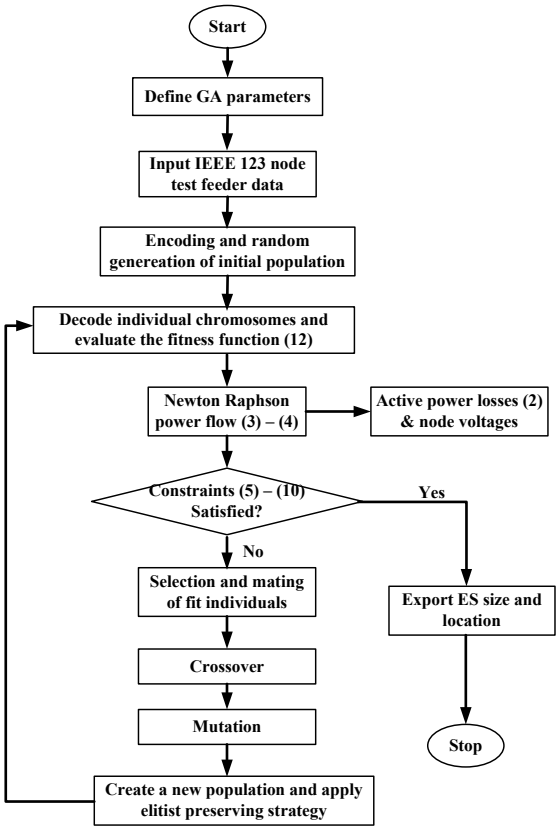

Fig. 1. Flowchart for the optimal size and site of the energy storage using GA

generation is formed at the end and the cycle is repeated again. A flowchart for the determination of the MW capacity and location of energy storage using the GA is displayed in Fig. 1. Whereas the flowchart is skewed towards the given IEEE 123 node test feeder, the approach presented herein is quite generic and can accommodate any test system configuration with any loading profile.

4. Test Results

The proposed method is tested on the IEEE 123 node test feeder of an actual 115 kV/4.16 kV 50-Hz distribution circuit [15]. The total load is modified to be 14 MW and is distributed among commercial and residential energy consumers.

The IEEE 123 node test feeder, shown in Fig. 2, consists of three-phase overhead or underground primary feeders and double-phase or single-phase line sections near the end of the feeder laterals. The 123 test feeder has 85 loads of different types, including constant current, constant impedance and constant power. The voltage at node 450, line 99 is monitored on hourly basis. That particular node is selected due its high voltage sensitivity. It is a point on the feeder that responds quickly to any changes in system conditions.

In this paper, it is assumed that the size and locations of the PV generation are determined solely by the PV owners (PVOs) based on resource availability and economic considerations. DSO has absolutely no control over its capacity and disposition in the system, as long as it complies with the host utility connection criteria and regulations. However, the DSO will utilize the ES to mitigate the intermittent nature of the PV generation.

The weighting factors were determined as $w_v = 0.55$ and $w_l = 0.45$ for voltage deviation and power losses respectively, after numerous simulation studies. Lower emphasis was given to the energy loss, as compared with the voltage, due to its dependency on voltage deviations. These weighting factors improve the overall system performance; in particular to streamline allocating the combination of the DES in two groups.

The proposed method has been realized in MATLAB, and examined on the IEEE 123 node test system for 24 hours using quasi-static time sequence analysis. The magnitude and location of the ES are found using the proposed GA-based optimization approach, as listed in Table 1. The single node location, amongst the 123 nodes, that corresponds to minimum voltage deviations and energy losses is node 81, when a 2.467 MW CES is connected to it. Similar results can be obtained when the DES are connected at nodes 81, 67, 78 and 91 respectively as listed in Table 1.

It is evident from the Table that, the proposed approach is capable of estimating the storage size at a single location or multiple locations with comparable sizes.

Table 1. GA results for the size and location of energy storage

Method	Centralized Energy Storage (CES)		Distributed Energy Storage (DES)	
	Bus	Rating (MW)	Bus	Rating (MW)
GA	81	2.467	81 67 78 91	1.247 0.915 0.100 0.235

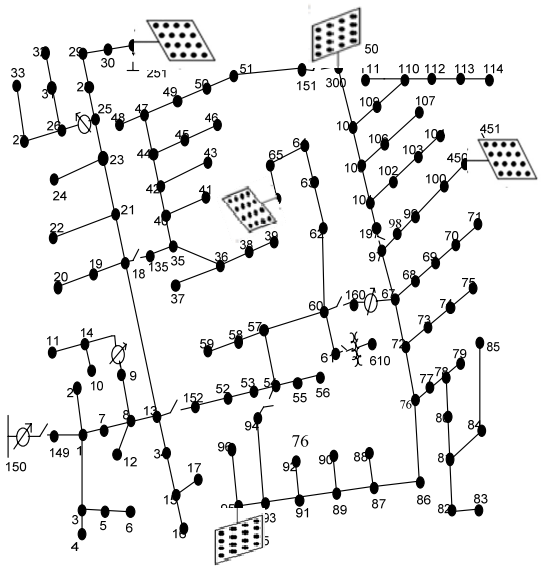

Fig. 2. IEEE 123 node test

4.1 Effect of distributed and centralized energy storage

Analysis of the 24-hourly simulation is carried out with a peak load of 14 MW and 30% solar PV penetration, connected as shown in Fig. 2. The voltage limits considered in this paper are +/- 6%. The voltage output of the feeder without ES is illustrated in a solid line in Fig. 3, with a minimum voltage of 0.943 pu and a maximum voltage of 1.01 pu.

Distributed energy storage (DES) is first considered in this scenario. The DES is distributed in the feeder according to their optimal locations and respective sizes determined by the GA, as listed in Table 1. The DES system is divided into two sections, since the maximum charging and discharging rate is 5 hours each. Section A comprises the ES at nodes 81 and 78, which are discharged between 2:00 to 7:00 hours and charged between 8:00 to 13:00 hours, as shown in Fig. 4. Section B consists of the ES integrated at nodes 67 and 91, which are discharged at the 1st hour of the day and between 20:00 to 24:00 hour and later charged between 14:00 to 18:00 hours, as demonstrated in Fig. 5.

The operation of the DES integrated with the PV generation in the feeder is marked with a dashed line in Fig. 3, with minimum voltage of 0.9585 pu and maximum

voltage of 0.9761 pu. Obviously, the DES has improved the voltage profile, especially when the voltage is low at night. Voltage deviations are minimized as well. Fig. 4 and Fig. 5 also depict the load shape curve in a dashed line. The 24-hourly energy loss during the charge and discharge operation of the DES is shown in a solid line in Fig. 6. The DES was able to reduce energy losses at most hours of the day, as demonstrated in Fig 3, and improve the voltage at night, corresponding to light load, when the voltage was close to the statutory level.

The second consideration dealt with centralized energy storage (CES). CES is now connected at a single optimal location determined by the GA, node 81, as listed in Table 1.

The penetration level of the solar-fueled PV and the peak load remain unchanged. The results are compared with the

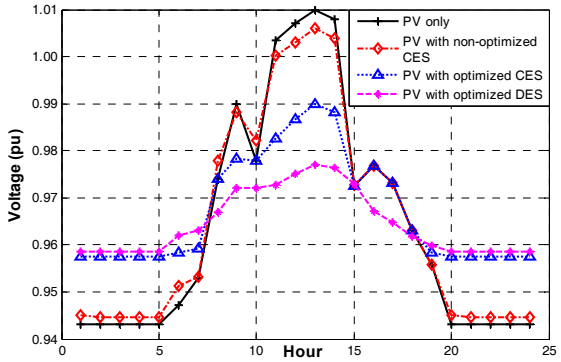

Fig. 3. Application of decentralized and centralized energy storage at 30% PV penetration at node 450

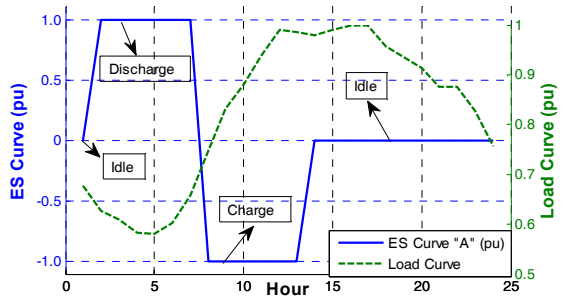

Fig. 4. Load and DES curve for section A

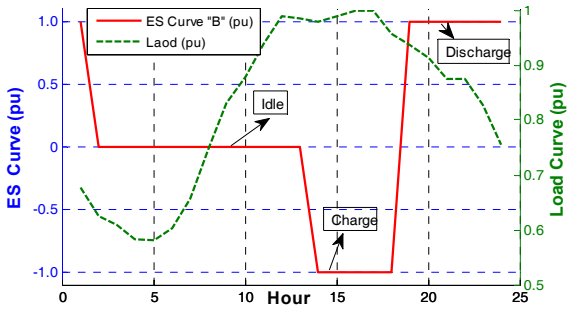

Fig. 5. Load and DES curve for section B

DES integration demonstrated earlier. The voltage profile of the system with the CES is depicted, in a dotted line, in Fig. 3. Furthermore, the significance of the optimized sizing and location of the ES is highlighted by contrasting it with the non-optimized centralized allocation of the ES as illustrated, in a dashed-dotted line, in Fig. 3. In that case, the same CES capacity of 2.467 MW is placed at node 42. It is blatantly clear, from Fig. 3, that the voltage profile is worse off than its counterpart of the optimized CES allocation at node 81.

The hourly losses during the charge and discharge operation of the CES are shown in a dashed line, in Fig. 6. It appears that the CES is slightly better in providing loss reduction. CES corresponds to a single optimized node location that brings the voltage deviations and energy losses to a minimum. Apportioning the ES is actually a tradeoff that renders suboptimal allocation of the DES into few nodes, producing less system losses. Nonetheless, DES is more effective in voltage rise mitigation, as shown in Fig. 3, PV output smoothing and load leveling than the CES, as demonstrated in Fig. 7. Furthermore, DES is better because of its flexibility and close proximity with consumers load.

The output voltage of the distribution system at 13:00 hour corresponding to some system nodes is depicted in Fig. 8. The peak load recorded at this hour of the day was 11.89 MW. The graph confers that, while improvement in the overall system voltage profile can be achieved on a diurnal basis, that improvement may not be necessarily true

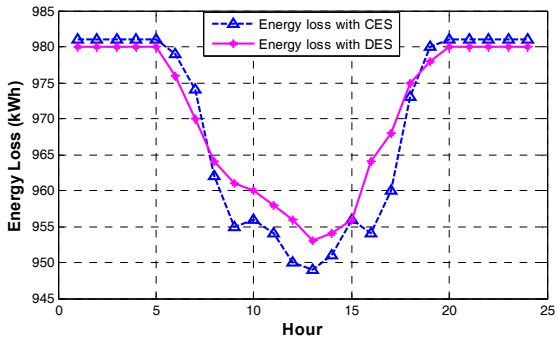

Fig. 6. 24-hourly energy loss of decentralized and centralized energy storage

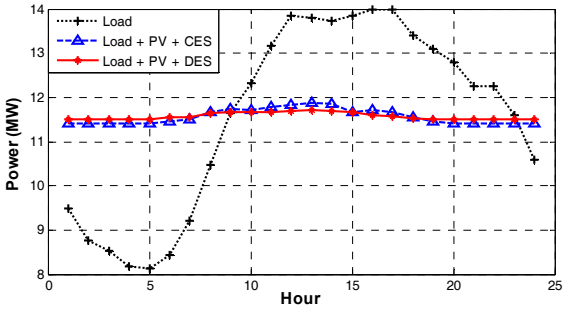

Fig. 7. Operation patterns of decentralized and centralized energy storage

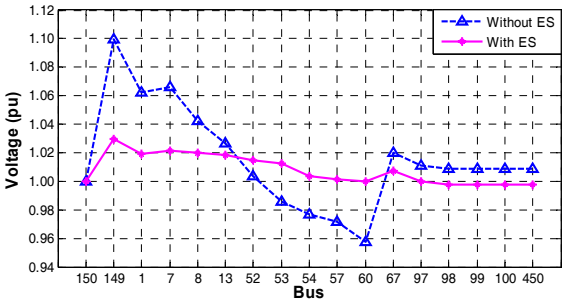

Fig. 8. Voltage magnitudes (pu) at some nodes

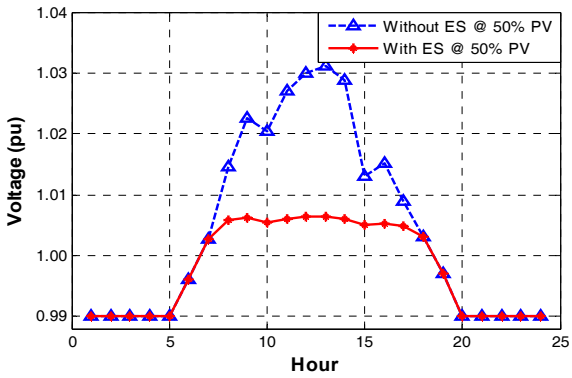

Fig. 9. The Effect of ES at 50% PV penetration at bus 450

for every hour of the day at all system nodes.

4.2 Effect of energy storage on high PV penetration

In this scenario, a peak load of 14 MW with 50% solar PV penetration is simulated on the IEEE 123 node test feeder. Application of the GA has determined the location and new size of the ES at this penetration level. The locations are the same but the sizes increase due to the increase in PV size.

The new sizes are 1.678, 1.138, 0.136, and 0.492 MW for node 81, 67, 78 and 91 respectively. The energy storage is energized to charge between 7th and 17th hour of the day, while in idle position in the remaining hours. In this case, while the ES on buses 81 and 72 are enabled to charge between 7th to 12th hours, ES on buses 67 and 91 charged between 12th and 18th hours. The voltage profile is as shown in Fig. 9. It is conspicuous that as the penetration increases, the ES becomes more useful. The ES is able to absorb the excess energy according to load demand to avoid energy spilling. It is thus able to mitigate the voltage rise due to high penetration of the PVs. This emphasizes, once more, the importance of the ES on the voltage control of distribution systems to accommodate higher levels of renewable generation.

4.3 Application of energy storage in solar PV curtailment

The output of a solar PV system can be affected due to

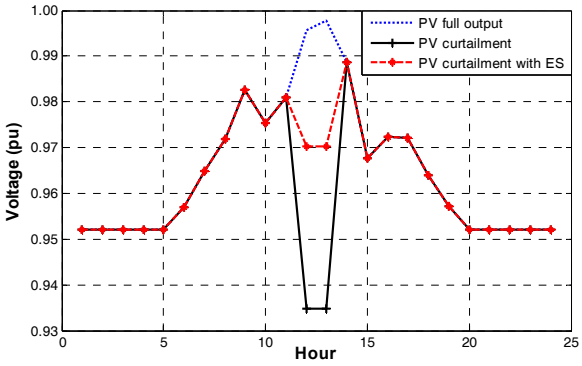

Fig. 10. Effect of energy storage on PV curtailment

cloud transients or partial shading or even energy spillage. The latter can occur when a large proportion of committed generation capacity comes from solar PV generation, giving rise to minimum load problems, as thermal generation cannot operate below certain output stage. In this case, the solar PV has to be curtailed. The implementation of ES can be flexibly used to expend any generation deficit/surplus and maintain electricity supply within statutory voltage limits at such period. It is also useful to avert extra ramping costs of thermal generation and opportunity costs of energy spillage.

A 25% PV penetration level, or 3.5 MW, is distributed at nodes 450, 300, 250, 95 and 79 on a 14 MW peak load feeder. The PV generators are curtailed between 12:00 and 13:00 hour of the day, at a peak period when needed most. It is assumed that these PVs are in the same geographical area and are subjected to similar geographical conditions. A 2.467 MW DES is distributed at the optimal positions, as illustrated in Table 1, in the feeder system. The 24-hourly simulation is carried out as manifested in Fig. 10. It appears that when the curtailment occurs, power output of the PVs plunges very rapidly, causing sudden voltage drop. ES discharges to increase the voltage profile from 0.9347 pu to 0.9703 pu during the period of curtailment. This highlights the effectiveness of the proposed GA-based method; particularly that, the energy storage did not only mitigate voltage rise, but also voltage drop as a result of solar PV curtailment.

5. Conclusions

Rapid integration of solar-fueled generation coupled with high penetration scenarios may potentially affect the operation of distribution systems. The intermittent characteristics of variable PV systems can result in voltage rise that can have adverse impacts on feeder circuits. Energy storage provides a buffer capacity to mitigate the variability of the PV generation. This paper has developed a GA-based mathematical programming approach to optimally find the size and strategic location of the energy storage needed, to maintain system-wide voltage within

permissible bounds. Using the time-integral part of the power flow analysis, quasi-static time sequence analysis is conducted over a 24 hours period. The proposed approach can effectively determine a centralized storage location or multiple locations for distributed storage.

The use of the energy storage, as illustrated in the paper, effectively assists to harness intermittent PV generation resources, mitigate voltage rise, bring further improvement to overall voltage profile, reduce thermal losses, provide capacity firming and PV output smoothing, and accommodate higher penetration levels of solar-fueled generation. Energy storage is poised to become an essential tool for grid support, leading to a higher synergy between customers and distribution networks encompassing large proportions of variable PV generation.

References

[1] Greg J. Shirek and Brian A. Lassiter, "Photovoltaic Power Generation: Modeling Solar Plants' Load Levels and Their Effects on the Distribution System," *IEEE Industry Applications Magazine*, vol. 19, no. 4, pp. 63-72, July/Aug 2013.

[2] Mesut E. Baran, Hossein Hooshyar, Zhan Shen, and Alex Huang, "Accommodating High PV Penetration on Distribution Feeders," *IEEE Trans. Smart Grid,* vol.3, no. 2, pp.1039-1046, June 2012.

[3] M. Thomson and D. G. Infield, "Impact of Widespread Photovoltaics Generation on Distribution Systems," *IET Renewable Power Generation*, vol. 1, no. 1, pp. 33-40, March 2007.

[4] Bradford P. Roberts and Chet Sandberg, "The Role of Energy Storage in Development of Smart Grids," *Proceedings of the IEEE*, vol. 99, no. 6, pp. 1139-1144, June 2011.

[5] Pedro M. S. Carvalho, Pedro F. Correia, and Luis A. F. M. Ferreira, "Distributed Reactive Power Generation Control for Voltage Rise Mitigation in Distribution Networks," *IEEE Trans. Power Systems*, vol. 23, no. 2, pp. 766-772, May 2008.

[6] Cody A. Hill, Mathew C. Such, Dongmei Chen, Juan Gonzalez, and W. Mack Grady, "Battery Energy Storage for Enabling Integration of Distributed Solar Power Generation," *IEEE Trans. Smart Grid*, vol. 3, no. 2, pp. 850-857, June 2012.

[7] J. O. Petinrin and Mohamed Shaaban, "Implementation of Energy Storage in a Future Smart Grid," *Australian Journal of Basic and Applied Sciences*, vol. 7, no. 4, pp. 273-279, March 2013.

[8] Francesco Marra, Y. Tarek Fawzy, Thorsten Bulo, and Bostjian Blazic, "Energy Storage Options for Voltage Support in Low-voltage Grids with High Penetration of Photovoltaic," *in Proceedings of IEEE PES ISGT Europe,* Berlin, Germany, Oct. 2012.

[9] Yasser M. Atwa and Ehab El-Saadany, "Optimal Allocation of ESS in Distribution Systems with a High Penetration of Wind Energy," *IEEE Trans. Power Systems*, vol. 25, no. 4, pp. 1815-1822, Nov 2010.

[10] Kwang Y. Lee and Mohamed A. El-Sharkawi, *Modern Heuristic Optimization Techniques: Theory and Applications to Power Systems*: John Wiley & Sons, 2008, p. 25-43

[11] C. Chen, S. Duan, T. Cai, B. Liu, and G. Hu, "Smart Energy Management System for Optimal Microgrid Economic Operation," *IET Renewable Power Generation*, vol.5, no.3, pp.258-267, May 2011.

[12] A. F. Crossland, D. Jones, and N. S. Wade, "Planning the Location and Rating of Distributed Energy Storage in LV Networks Using a Genetic Algorithm with Simulated Annealing," *International Journal of Electrical Power & Energy Systems*, vol. 59, pp. 103-110, July 2014.

[13] Mohamed Shaaban and J. O. Petinrin, "Sizing and Siting of Distributed Generation in Distribution Systems for Voltage Improvement and Loss Reduction," *International Journal of Smart Grid and Clean Energy*, vol.2, no.3, pp.350-356, Oct 2013.

[14] Jared L. Cohon, and David H. Marks, "A Review and Evaluation of Multiobjective Programming Techniques," *Water Resources Research*, vol. 11, no. 2, pp. 208-220, April 1975.

[15] W. H. Kersting, "Radial Distribution Test Feeders," *IEEE Trans. Power Systems*, vol.6, no.3, pp.975-985, Aug 1991.

Mohamed Shaaban He received his B.Sc. (honors) and M.Sc. degrees from Suez Canal University, Egypt and his Ph.D. degree (all in Electrical Engineering) from the University of Hong Kong in 1990, 1996, and 2002 respectively. His research interests include power system operation, optimization, risk analysis, distributed generation, renewable energy integration and smart grids. Dr. Shaaban is a Chartered Engineer, UK and a Senior Member, IEEE.

J. O. Petinrin He received his M.Eng. degree in Electrical Engineering from the Federal University of Technology, Akure, Ondo State, Nigeria in 2007. He received his Ph.D. degree in Electrical Engineering from Universiti Teknologi Malaysia (UTM), Johor Bahru, Malaysia in 2015. His research interests include renewable energy and voltage control of distribution systems.